

Effect of SiC particles on microstructure and mechanical property of friction stir processed AA6061-T4

Don-Hyun CHOI¹, Yong-Il KIM², DAE-Up KIM³, Seung-Boo JUNG^{1,2}

1. School of Advanced Materials Science and Engineering, Sungkyunkwan University, 300 Cheoncheon-dong, Jangan-gu, Suwon, Gyeonggi-do 440-746, Korea;
2. MEPL, Sungkyunkwan University, 300 Cheoncheon-dong, Jangan-gu, Suwon, Gyeonggi-do 440-746, Korea;
3. KITECH, 838-11, Palbok-dong 2-ga, Deokjin-gu, Jeonju-city, Jeollabuk-do 561-844, Korea

Received 21 May 2012; accepted 9 October 2012

Abstract: Friction stir processing of AA6061-T4 alloy with SiC particles was successfully carried out. SiC particles were uniformly dispersed into an AA6061-T4 matrix. Also SiC particles promoted the grain refinement of the AA6061-T4 matrix by FSP. The mean grain size of the stir zone (SZ) with the SiC particles was obviously smaller than that of the stir zone without the SiC particles. The microhardness of the SZ with the SiC particles reached about HV80 due to the grain refinement and the distribution of the SiC particles.

Key words: friction stir processing; AA6061-T4; SiC particles; pinning effect

1 Introduction

Good strength-to-mass ratio, high thermal conductivity, and good corrosion resistance have made aluminum alloys very popular as structural materials. However, their relatively poor wear resistance has limited their tribological applications. The use of ceramic particles, such as silicon carbide and aluminum oxide, as reinforcements to form aluminum matrix composites have been well studied [1–5]. Recent research has demonstrated that, for a fixed concentration, smaller particles usually produce stronger and harder composites [5]. This finding has led to a number of studies on developing nano- or sub-micro-particles reinforced aluminum composites. These have mostly involved either casting or powder metallurgy (PM) processes. For cast composites, the particle volume fraction is limited to 2% (volume fraction) [6,7] because the low density of the nano- or sub-micro-powder causes it to occupy a large space, making it difficult to add into melted metal. Although a substantial increase in strength has been observed in low particle concentration cast composites, enhancement of wear resistance has been limited.

Previous study shows that PM processes involving mixing by ball milling, successfully produced Al–Al₂O₃ composites with particle concentrations of up to 30% (volume fraction) [8]. Promising tribological properties were demonstrated. However, these PM processes are costly and as such have restricted the part sizes and geometries of the final product. In addition, the high ceramic concentration significantly reduces the ductility and thermal conductivity of the material.

Recently, much attention has been paid to the friction stir processing (FSP) for its promise as a solid-state surface modification technique [9–11]. A rotating tool with a specially designed pin and shoulder is inserted into a substrate and produces a highly plastically deformed zone (stir zone). It is well known that the stir zone consists of fine and equiaxed grains produced by dynamic recrystallization [11]. FSP has also been used to fabricate surface composites. MISHRA et al [11] fabricated Al/SiCp surface composites by FSP, they showed that SiC particles were well distributed in the Al matrix and good bonding with the Al matrix was obtained. As the processing of the surface composite during FSP is carried out at temperatures below the melting point of the substrate, problems seen in

conventional techniques based on liquid phase processing at high temperatures can be avoided.

Therefore, in this work, the effect of SiC particles on the microstructure, powder distribution pattern, microhardness values of friction stir processed AA6061-T4 was investigated.

2 Experimental

The base metal (BM) used in this work was the AA 6061 alloy with 4 mm thickness rolled plates. It was heat-treated and naturally aged to a T4 stable condition. This alloy, in the T4 condition, has good hemming properties, good weldability, very good corrosion resistance and formability with no stretcher strain marks. AA6061 is a typical commercial alloy containing (mass fraction) 0.92% Mg, 0.57% Si and a very small amount of the other additives. This material is commonly used in aircraft, automobile, shipbuilding and other pressured vessels. The tool rotation rate was set to 1600 r/min, and its advancing speed was 80 mm/min.

A groove with a depth and width of 1 and 2 mm was machined out of the AA6061 workpieces for inserting the SiC particles. A schematic illustration of the FSP setup is shown in Fig. 1. In order to prevent sputtering of the powders and their ejection from the groove during processing, the groove was initially closed by aluminum

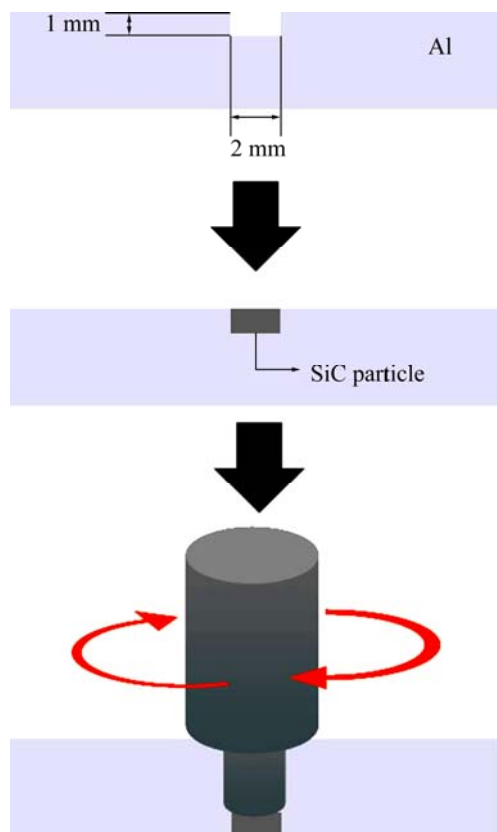


Fig. 1 Schematic illustration of FSP process of AA6061-T4 with SiC particles

tape. At first, the back side is FSPed and the front side is welded after the strip of aluminum tape. All FSP experiments were carried out at room temperature using a double pass method (back side and from side).

As-processed workpieces were cut transverse to the FSW direction, mechanically polished, and etched with Keller's reagent (1 mL hydrofluoric acid, 1.5 mL hydrochloric acid, and 2.5 mL nitric acid in 95 mL distilled water). Microstructural changes were observed by employing optical microscopy (OM) and scanning electron microscopy (SEM) at the cross sections perpendicular to the FSP direction.

The Vickers hardness profile of the joint was measured at the cross section and perpendicular to the welding direction using a Vickers indenter with a 0.98 N load for 10 s.

3 Results and discussion

Figure 2 shows the optical macrostructure and the related microstructures of each region indicated in the macrostructure. The SZ is wider near the upper surface than around the lower surface producing a semi-sphere shape because the upper surface experiences extreme deformation and frictional heat caused by direct contact with the welded plates of the cylindrical tool shoulder. Local variation of the microstructure can be seen because each SZ experienced different thermomechanical conditions [12]. Macroscopic examination of the SZ reveals a relative non-symmetric shape that is mainly associated with the tilt angle of the tool and the relation between the tool rotation direction and the welding direction [13]. It is apparent that the SZ exhibits a high degree of continuity and is not porous. Unlike that of the base metal (BM, Fig. 2(a)), the SZ (Fig. 2(b)) has fine and equiaxed grains and the grain size is much smaller than that of the BM. This structure was showed dynamic recrystallization and static grain growth after welding, this was caused by frictional heat and plastic deformation [14,15]. It is evident that the original grain structure was microscopically upset in the thermo-mechanically affected zone (TMAZ, Fig. 2(c)) and a transient microstructure between the SZ and heat affected zone (HAZ, Fig. 2(d)) was obtained. The elongated and dynamic recovered grain structure is characterized in TMAZ because of the thermal and deformation conditions were not sufficient to produce a recrystallized grain structure [16]. The HAZ has a similar grain size to the unaffected BM. The mechanical conditions and temperature in the HAZ were not sufficient to promote grain growth or macroscopically to deform the BM.

The optical macro and microstructure of the FSPed AA6061-T4 with SiC particles is shown in Fig. 3. In spite of the groove, no cracks or defects are observed in

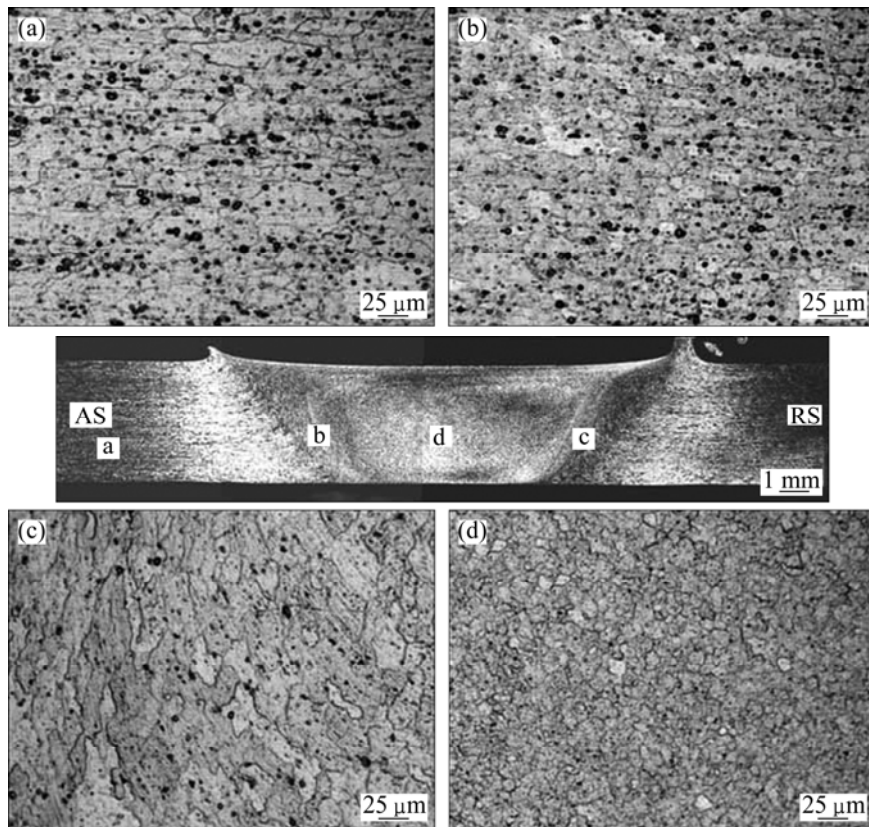


Fig. 2 Optical macro cross-sectional image and microstructure in each region of FSPed AA6061-T4 without SiC particles: (a) BM; (b) SZ; (c) TMAZ; (d) HAZ

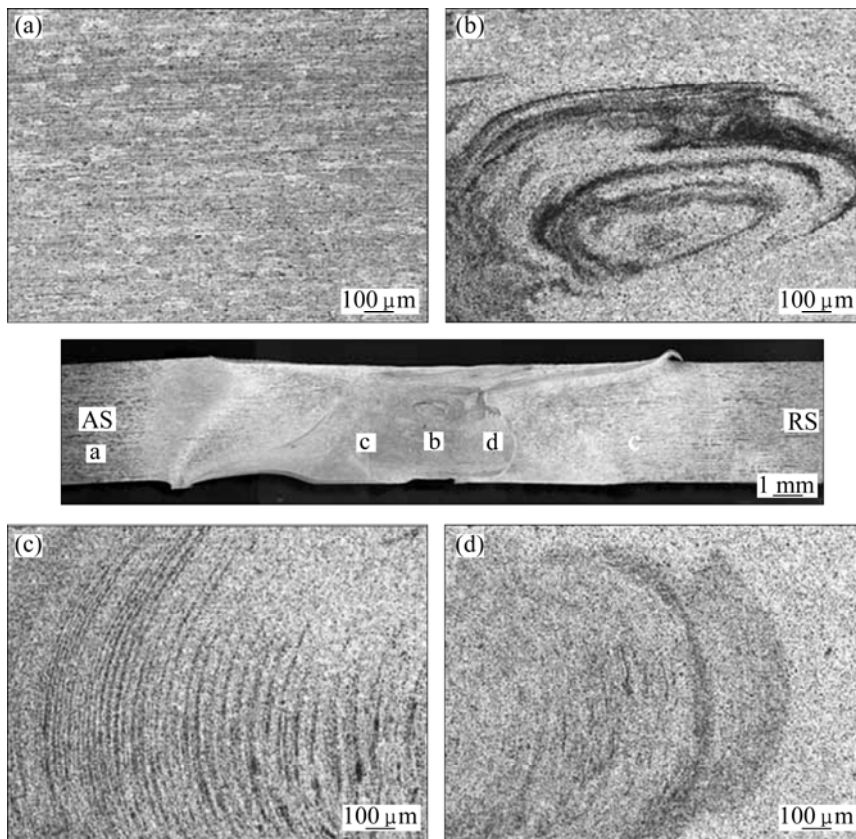


Fig. 3 Optical macro cross-sectional image and microstructure in each region of FSPed AA6061-T4 without SiC particles: (a) BM; (b) SZ; (c) TMAZ(AS); (d) TMAZ(RS)

the SZ. The SZ shape is nearly the same as the SZ without SiC particles, but some black lines observed in the SZ. It seems that the black lines are related with the distribution of SiC particles. In the TMAZ, SiC particles are distributed along some parallel bands in the matrix (Figs. 3(b)–(c)).

FSP also led to grain refinement of the Al matrix, as can be seen by comparing the microstructures for SZ without SiC particles and SZ with SiC particles, as seen in Fig. 4. The microstructure of the BM is shown in Fig. 4(a), its grain size is about 30 μm . Figure 4(b) shows the microstructure of the SZ without SiC particles. The grain size is about 15 μm in this region. The phenomenon which causes thermo-mechanically processed materials to have very small grains is called dynamic recrystallization. During this process, material undergoes severe plastic deformation. During plastic deformation, the grains are broken and a large number of low-angle misorientated grain boundaries are created; furthermore highly favorable locations for nucleating recrystallization are produced. During dynamic recrystallization (DRX) low angle boundaries transform to high angle ones and

nucleation of new grains at preferential sites takes place. Then, the fine nuclei of grains start growing and finally a microstructure containing fine equiaxed grains are created. Fine-grain microstructures have large areas of grain boundary and therefore have a large amount of stored energy. As such, they are inherently susceptible to grain growth during high-temperature deformation. Therefore, when approaching the lowest level of energy, new fine grains start growing. The dispersion of SiC particles help to prevent this grain growth, grain size of SZ with SiC particles is decreased to 3 μm . The pinning effect of SiC particles during grain growth impedes the migration of grain boundaries. Decreasing the particle size intensifies the pinning of the grain boundary due to the larger number of particles in the same volume fraction. In addition, it is worth mentioning that SiC particles cause inhomogeneous local deformation that assists the break-up of the grains. Consequently, it can be concluded that the decreasing the size of the SiC particles: increases the nucleation sites, intensifies the pinning effect of particles and increases the break-up of pre-existing grains.

Figures 5(a)–(c) show the SEM micrographs of the microstructure of the SZ, TMAZ at AS and RS with SiC particles. The TMAZ, where both thermal and plastic deformation effects were evident, is composed of SiC particles and recrystallized grains. The former have an obvious orientation along the metal-flow direction induced by stirring. In the SZ, the original microstructure of the BM changed to a fine recrystallized grain structure, and SiC particles were homogeneously distributed in the Al matrix due to plastic deformation and stirring. Also by comparing the amount of SiC particles in the TMAZ between AS and RS, we get further confirmation this phenomenon is explained by material flow. It is well known that material flow occurs from RS to AS during FSW. Considering this result, it seems that SiC particles in the groove at the center of the specimens were differently distributed between AS and RS, and more SiC particles were distributed at AS than at RS. However, it is worth noting that the SiC particles existed in all three zones, i.e., the SZ, TMAZ at AS and RS, although their volume fraction differed.

Hardness profiles of the FSPed AA6061-T4 with and without SiC particles are shown in Fig. 6. FSPed sample without SiC particles has homogeneous hardness profiles. Its average hardness value is about HV55, which is identical to that of the T4 B. No change in the hardness profiles suggests that the re-precipitation of the stable or metastable precipitates does not occur during the welding, since the precipitation is sensitive to the hardness values in precipitation-hardenable Al alloys. However, in the SZ with SiC particles, we can see that the hardness of the SZ was higher than that of the BM;

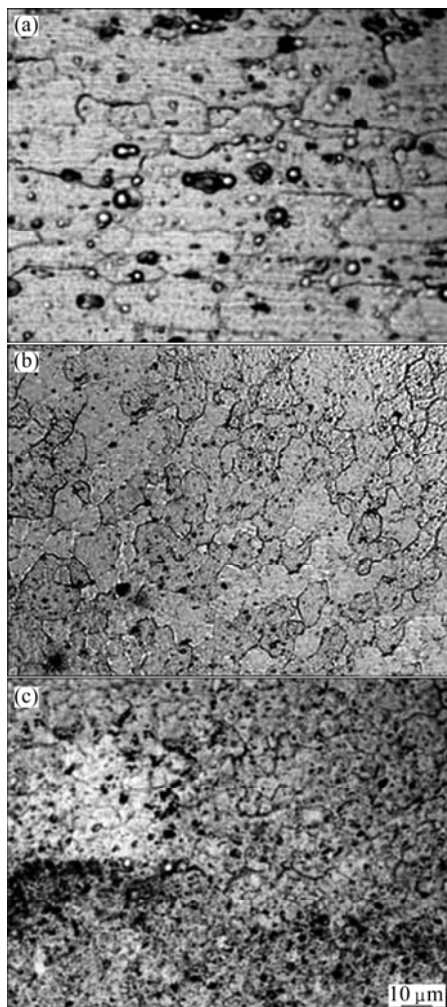


Fig. 4 Optical microstructures of each regions: (a) BM; (b) SZ without SiC particles; (c) SZ with SiC particles

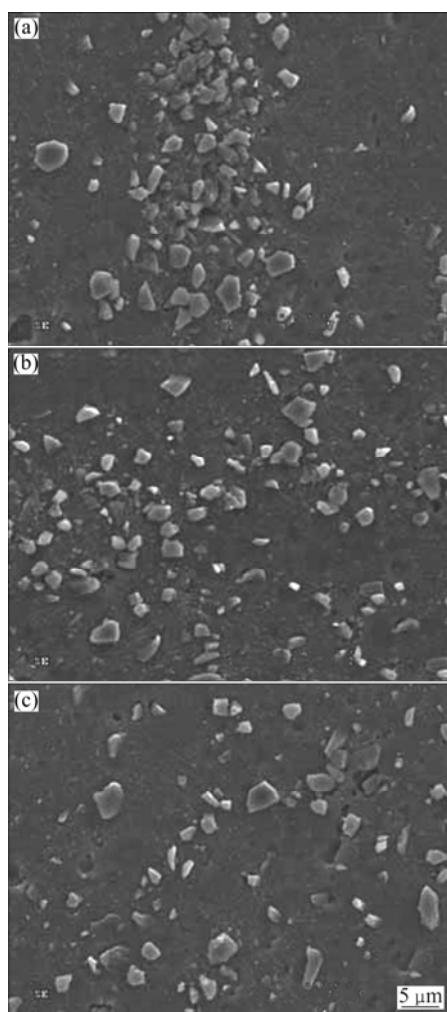


Fig. 5 SEM micrographs of each regions in FSWed AA6061-T4 with SiC powders: (a) TMAZ (AS); (b) SZ; (c) TMAZ(RS)

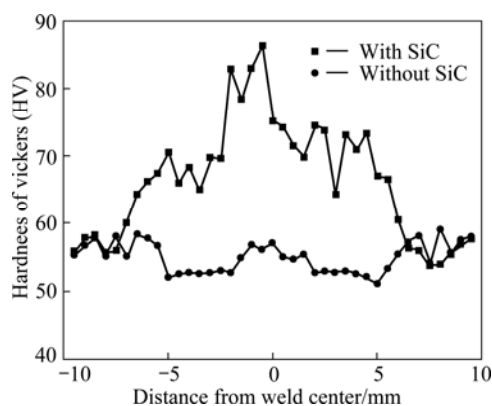


Fig. 6 Distribution of Vickers hardness of FSPed AA6061-T4 with and without SiC particles

the average hardness values of the SZ are HV 75. We believe that the improvement in the hardness of the SZ is related to the grain size and presence of SiC particles. Firstly, the grains of the SZ were finer than those in the BM and it is well known that fine grains play an important role in strengthening a material. Secondly, the small SiC particles also contributed to increasing the

hardness due to dispersion strengthening mechanism.

4 Conclusions

1) Fabricated composite material with SiC particles in AA6061-T4 were produced successfully by FSP.

2) In the SZ, the original microstructure of the BM changed to a fine recrystallized grain structure, and SiC particles were homogeneously distributed in the Al matrix due to mechanical stirring.

3) The mechanical property such as hardness of the SZ is improved by reducing of grain size and dispersed SiC particles.

References

- [1] ALPAS A T, ZHANG J. Effects of microstructure (particulate size and volume fraction) and counter face material on the sliding wear resistance of particulate reinforced aluminum matrix composites [J]. *Metallurgical and Materials Transactions A*, 1994, 25: 969–983.
- [2] SANNINO A P, RACK H. Dry sliding wear of discontinuously reinforced aluminum composites: Review and discussion [J]. *Wear*, 1995, 189: 1–19.
- [3] DEUIS R L, SUBRAMANIAN C, YELLUP J M. Dry sliding wear of aluminum composites—A review [J]. *Composites Science and Technology*, 1997, 57: 415–435.
- [4] GUSTAFSON T W, PANDA P C, SONG G, RAJ R. Influence of microstructural scale on plastic flow behavior of metal matrix composites [J]. *Acta Materialia*, 1997, 45: 1633–1643.
- [5] KOUZELI M, MORTENSEN A. Size dependent strengthening in particle reinforced aluminum [J]. *Acta Materialia*, 2002, 50: 39–51.
- [6] WU J M, LI Z Z. Nanostructured composites obtained by mechanically driven reduction reaction of CuO and Al powder mixture [J]. *Journal of Alloys and Compounds*, 2000, 299: 9–16.
- [7] ZHANG H, MALJKOVIC N, MITCHELL B S. Structure and interfacial properties of nanocrystalline aluminum/mullite composites [J]. *Materials Science and Engineering A*, 2002, 326: 317–323.
- [8] AL-QUTUB A M, ALLAM I M, ABDUL SAMAD M A. Wear and friction of Al-A1203 composites at various sliding speeds [J]. *Journal of Materials Science*, 2008, 43: 5797–5803.
- [9] MA Z Y, SHARMA S R, MISHRA R S. Microstructural modification of as-cast Al–Si–Mg alloy by friction stir processing [J]. *Metallurgical and Materials Transactions A*, 2006, 37: 3233–3236.
- [10] SHARMA S R, MISHRA R S. Fatigue crack growth behavior of friction stir processed aluminium alloy [J]. *Scripta Materialia*, 2008, 59: 395–398.
- [11] MISHRA R S, MA Z Y. Friction stir welding and processing [J]. *Materials Science and Engineering R*, 2005, 50: 1–78.
- [12] LIU G, MURR L E, NIOU C S, MCCLURE J C, VEGA F R. Microstructural aspects of the friction-stir welding of 6061-T6 aluminum [J]. *Scripta Materialia*, 1997, 37: 355–361.
- [13] THOMAS W M, NICHOLAS E D. Friction stir welding for the transportation industries [J]. *Materials & Design*, 1997, 18: 269–273.
- [14] SATO Y S, KOKAWA H, IKEDA K, ENOMOTO M, JORGAN S, HASHIMOTO T. Microtexture in the friction-stir weld of an aluminum alloy [J]. *Metallurgical and Materials Transactions A*, 2001, 32: 941–948.
- [15] JATA K V, SEMIATIN S L. Continuous dynamic recrystallization during friction stir welding of high strength aluminum alloys [J]. *Scripta Materialia*, 2001, 43: 743–749.
- [16] SU J Q, NELSON T W, MISHRA R S, MAHONEY M. Microstructural investigation of friction stir welded 7050-T651 aluminium [J]. *Acta Materialia*, 2003, 51: 713–729.

(Edited by YANG You-ping)